ISSN 1028-6845
BGJ
BANGLADESH GEOSCIENCE JOURNAL VOL. 27, P. 17-41, 2021

Textural and heavy mineral characteristics of the bar sediments from the upper reaches of the Atrai River, northwest Bangladesh

ABU SADAT MD. SAYEM[1*], KH. FARZANA ZOHA[1], MD. ROKONUZZAMAN[1], MD. JOYNUL ABEDEN[1,2] & ZAHIDUL BARI[1]

Abstract

The Atrai River originates in the southeast of the Himalaya and is considered one of the major tributaries of the mighty Brahmaputra River in the Bengal Basin. This paper presents the textural and heavy mineral distribution of the bar deposits from the upper reaches of the Atrai River. The textural characteristics suggest that the Atrai River sediments are medium- to fine grained (avg.1.47φ), moderately well sorted (avg.0.58φ), positively skewed (~78%) and mesokurtic to leptokurtic in nature. Various bivariate diagrams indicate the investigated sediments were deposited in the channel floor under a medium level of energy. The results also suggest that the sediments are mostly bedload sediments and were deposited by rolling and suspension mechanisms. The heavy mineral analysis reflects the predominance of metastable heavy minerals (garnet, epidote, staurolite, kyanite, and sillimanite) than the ultra-stable heavy minerals (zircon, rutile, and tourmaline). A low- to high-grade metamorphic source terrain is suggested by the heavy mineral suite of garnet, epidote, kyanite, staurolite, and sillimanite. An acid igneous source complex is reflected by the occurrence of zircon, rutile, tourmaline, apatite, and hornblende. A basic igneous rock provenance is indicated by the presence of pyroxene and opaque minerals. Occurrences of rounded to sub-rounded zircon and rutile indicate sedimentary and meta-sedimentary provenance. Thus, it appears that the Atrai River sediments were derived from mixed sources, likely from the eastern part of the Higher Himalaya, the Lesser Himalaya and the southeasterly Sub-Himalayan Ranges.

Keywords: Atrai River, Bengal Basin, Heavy mineral, Sedimentary Processes, Provenance.

Introduction

Grain size is one of the important descriptive properties of siliciclastic sedimentary rocks. The sizes of particles in a particular deposit reflect weathering and erosion processes, which generate particles of various sizes, and the nature of subsequent transport processes (BOGGS 2001). The size composition of sediment is controlled by hydrodynamic conditions prevailing during deposition (UDDEN 1914). The sediment size and uniformity of grain size or sorting are measures of the

Authors' Addresses: ABU SADAT MD. SAYEM[1*], KH. FARZANA ZOHA[1], MD. ROKONUZZAMAN[1], MD. JOYNUL ABEDEN[1,2] & ZAHIDUL BARI[1], [1]Department of Geological Sciences, Jahangirnagar University, Dhaka 1342, Bangladesh, [2]ACE Consultant Ltd., Baridhara, Dhaka 1212, Bangladesh. *Email: sayem8282@juniv.edu*

competence and efficiency of the transporting agent. Grain size distribution and textural parameters give useful information about the environment as they reflect the mode of transportation, deposition, and relation between size and distance (FRIEDMAN 1961).

Many workers have been trying to establish different depositional environments based on grain size parameters for several years (FOLK & WARD 1957; FRIEDMAN 1961, 1967 & 1979; MASON & FOLK 1958; PASSEGA 1957 & 1964; PASSEGA & BYRAMJEE 1969; SING *et al*. 2007; KANHAIYA *et al*. 2017). FOLK & WARD (1957), MASON & FOLK (1958), and FRIEDMAN (1961, 1967 & 1979) have used the statistical parameters of mean, standard deviation and skewness to deduce the depositional environment of clastic sediments. FRIEDMAN (1967) introduced different graphic measurements, known as the simple sorting measure and the simple skewness measure, which included distinguishing between beach, dune, and river sediments. PASSEGA (1957 & 1964) and PASSEGA & BYRAMJEE (1969) have attempted to establish the relationship between textural and depositional processes, rather than between texture and environment, and use the relationships between certain sizes and the most probable depositional mechanism to classify clastic sediments by subdividing them into types indicative of their genesis. KANHAIYA *et al*. (2017) used the graphic mean and sorting relationships to separate the channel and floodplain deposits. SING *et al*. (2007) showed the modes of sediment transport mechanisms using skewness and sorting parameters.

Minerals with specific gravities greater than 2.9 are known as heavy minerals. Heavy mineral concentrations are very low and vary widely in igneous, metamorphic, and sedimentary rocks. In addition, heavy minerals are very resistant to chemical weathering and travel a long distance before being deposited. Thus, the heavy minerals are good indicators for provenance study. However, most of the heavy minerals have economic significance. Besides beach environments, fluvial sand bars are suitable places for heavy mineral concentrations.

There have been numerous recent sedimentological studies on the geochemistry and heavy minerals from the major rivers of Bangladesh (the Jamuna, the Ganges, Meghna, the Teesta) (SAYEM & RAHMAN 2012; ABEDEN *et al*. 2017; ALI *et al*. 2019; HOSSAIN 2019; RAHMAN *et al*. 2020a, 2020b; RAHMAN *et al*. 2021; RAHMAN *et al*. 2022). The textural properties of the bar deposits from the upper reaches of the Bengal Basin rivers, however, are not well understood. In addition, grain size distribution and heavy mineral studies are rare in the channel bars of the Atrai River sediments. This study aims to define the textural distribution and heavy mineral assemblage of the bar deposits from the Atrai River northwest Bangladesh in order to define the sediment dynamics and source rock composition in the provenance.

Geological setting of the study area

Formerly, the Atrai River was one of the largest rivers in the northwest Bengal Basin and served as the main channel by which the waters of the Teesta River discharged into the Ganges. But in 1787, the Teesta River broke away from its ancient bed and carved out for itself a large new route through which it entered the Brahmaputra. The Atrai River originates in Shiliguri District of West Bengal, passes through the Dinajpur district of Bangladesh, enters India once more, flows past the Chalan Bil, and eventually empties into the Jamuna (Brahmaputra) River (Fig. 1a). At present, the Atrai, one of the main channels of the Teesta Alluvial Fan, is located between 25°18'13" N and 26°42'50" N and 88°30'44" E and 88°45'19" E.

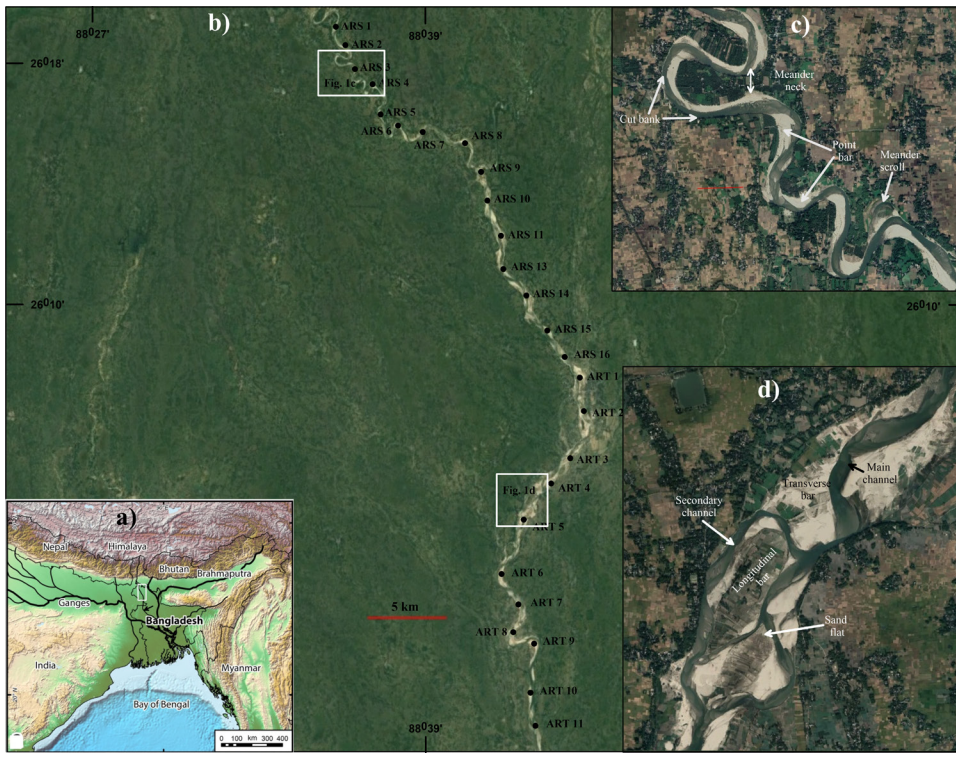

Fig. 1. **a**) Location map of the Atrai River and surrounding regions (the black arrow indicates the course of the Atrai River and white rectangle indicates the study area); **b**) sampling point location map of the study area; **c**) meander belts and geomorphic units of the Atrai River; **d**) braided geomorphic units of the Atrai River.

The Bengal Basin has originated due to the collision between the Indian and the Eurasian plates in north and with the Burmese plate in east, and resulted the extensive Himalayan and Indo-Burman Ranges and thereby loading the lithosphere to form flanking sedimentary basins (UDDIN & LUNDBERG 1998). Due to decreasing trend of

elevation from north to south, almost all of the rivers in the Bengal Basin flow from north to south direction. Tectonically, the Atrai River lies in the Stable Platform of the Bengal Basin. It flows southward along the axial plain of the Teesta Alluvial Fan at its upper reaches (Fig. 1b). The lower reaches of the river crosses over the Pleistocene Barind Tract and unconsolidated Holocene Alluvium of the Ganges and Brahmaputra floodplain until its confluence with the Brahmaputra River. Geomorphologically, the Atrai River is dominantly braided in nature (Fig. 1d), but also shows meandering nature in places (Fig. 1c). At present, the total length of the Atrai River is approximately 390 km and the maximum depth is about 30 ft.

Methodology

For the purpose of this study detail field work has been carried out in the upstream of the Atrai River in Bangladesh territory (Fig. 1a, b) immediately after the rainy season (as the cut bank erosion is rapid) in 2014 and 2019. The sediment samples were collected from the channel bar deposits at a regular interval of approximate 3 km and at a considerable depth of about 50 cm. Hand auger has been used to collect the samples. Raw and wet samples were preserved in the polyethylene bags and brought to the laboratory for analysis. A total of 27 sediment samples were collected for laboratory investigation.

In this study, grain size analysis has been performed to discriminate the sediment depositional processes and mechanisms. For this analysis about 100 gm of each dried sample was taken and sieved by "Ro–Tap sieving machine" for 15 minutes using 18, 35, 60, 120 and 230 U.S. standard meshes and their size distributions were recorded. The grain size parameters were obtained according to FOLK & WARD (1957). All the samples were analyzed at the Department of Geological Sciences, Jahangirnagar University, Dhaka, Bangladesh.

19 samples were selected for heavy mineral analysis. The sediment sizes of 1 mm to 0.063 mm were used for heavy mineral separation. 10 gm of each sample were run for the gravity separation by using Bromoform ($CHBr_3$) (density is 2.89 gm/cc at 20°C) following the procedure outlined by MANGE & MAURER (1992). The light and heavy fractions were weighed and their weight percentages were calculated. After drying the heavy minerals are mounted on standard microscope glass slides by using Canada balsam. After preparing, the slides were observed under polarizing microscope (Motic PM-18 series, Meiji ML 9000) and at least 200 grains were counted using ribbon counting method. Photographs of the representative heavy minerals were taken using a digital camera attached to a high level research polarizing microscope at the Wazed Miah Research Center, Jahangirnagar University, Dhaka, Bangladesh.

Results

Textural parameters

Various grain size parameters, such as graphic mean, sorting, skewness and

kurtosis, were used to evaluate depositional environment of sediments. These parameters are calculated using the formula after FOLK & WARD (1968). The graphical representation of the grain size data is the most important and meaningful method for understanding the environments of deposition of sediments (FOLK 1968). The statistical parameters of the Atrai River sediments are tabulated in the Table 1 and described as follows:

Table 1. Results of the statistical parameters of the sediments from the upper reaches of the Atrai River.

Sample No.	Mz (φ)	SD (φ)	Sk	Kg	M (φ)	C (φ)
ARS-01	2.55	0.65	-0.32	1.50	2.70	0.30
ARS-02	1.83	0.53	0.13	0.77	1.80	0.28
ARS-03	2.17	0.66	-0.06	1.06	2.20	0.23
ARS-04	1.53	0.54	0.40	0.96	1.40	0.21
ARS-05	1.60	0.56	0.15	0.82	1.60	0.06
ARS-06	1.35	0.58	0.03	1.17	1.36	0.03
ARS-07	1.33	0.54	0.23	1.13	1.30	0.09
ARS-08	1.40	0.40	-0.06	1.15	1.45	0.15
ARS-09	1.07	0.33	0.11	1.46	1.06	-0.03
ARS-10	1.07	0.50	0.16	1.60	1.00	-0.21
ARS-11	1.30	0.48	0.37	1.09	1.20	0.06
ARS-12	1.57	0.60	0.13	0.96	1.50	0.06
ARS-13	1.48	0.56	0.33	0.95	1.36	0.06
ARS-14	1.48	0.66	0.12	0.93	1.45	0.23
ARS-15	1.30	0.48	0.30	1.13	1.20	0.00
ARS-16	1.50	0.51	0.31	1.02	1.40	0.12
ART-01	1.51	0.67	-0.02	0.99	1.48	0.16
ART-02	1.3	0.47	0.03	0.82	1.30	0.00
ART-03	1.65	0.67	-0.26	0.85	1.75	0.75
ART-04	1.17	0.61	0.23	1.02	1.10	0.13
ART-05	1.24	0.76	0.31	0.6	1.10	0.00
ART-06	1.61	0.53	0.14	0.85	1.55	0.72
ART-07	1.16	0.63	0.08	1.29	1.10	-0.30
ART-08	1.68	0.53	0.09	1.24	1.60	1.30
ART-09	1.48	0.71	0.15	0.82	1.40	0.91
ART-10	0.95	0.78	-0.05	1.63	0.93	0.92
ART-11	1.52	0.63	0	0.96	1.50	0.56
Average	**1.47**	**0.58**	**0.11**	**1.07**	**1.44**	**0.27**

Mz- mean, SD-standard deviation, Sk- skewness, Kg-kurtosis, M-median, C-1 percentile

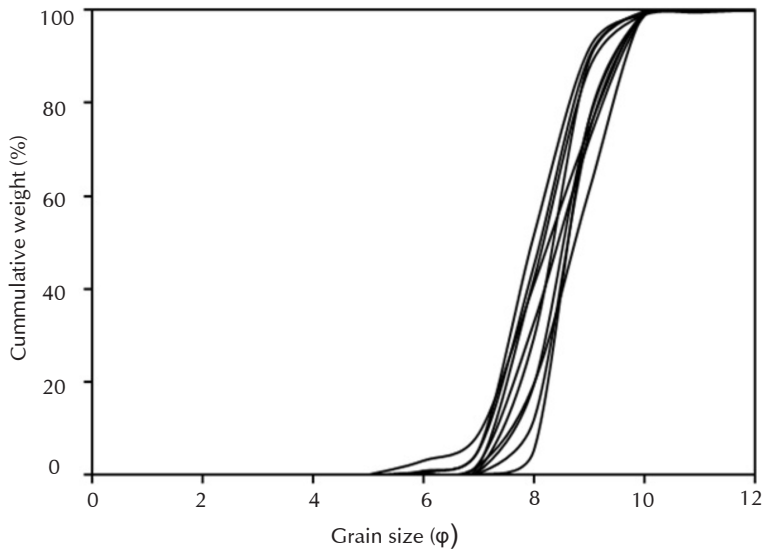

Fig. 2. Cumulative frequency curve of the Atrai River sediments.

Graphic mean (Mz)

Mean value indicates the relative size of clastic grains (BOGGS 2009). The Atrai River sediments show a variable mean size range between 2.55φ and 0.95φ (Table 1). The average of mean value of the investigated samples is 1.47φ, indicating the excess of medium grained sand. The predominance of medium grained sediments also reflected moderate-energy condition of deposition in the Atrai River basin. The spatial distribution shows that the mean size of the Atrai River sediments decreases downstream (Fig. 3).

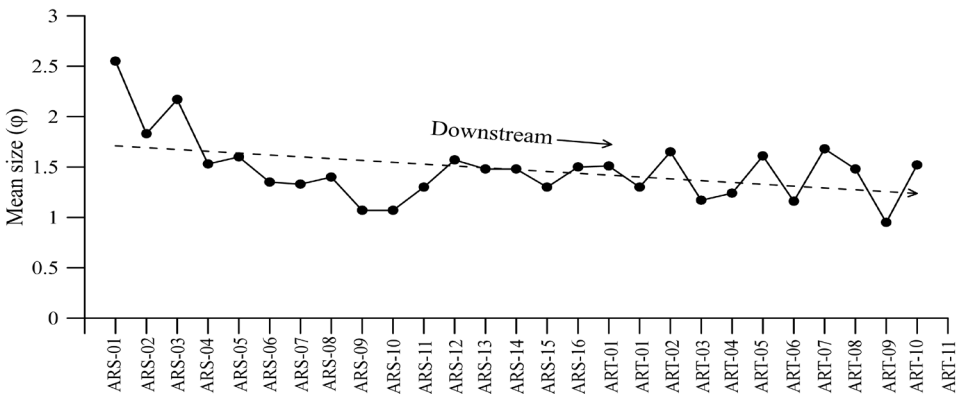

Fig. 3. Spatial distribution of mean size of the Atrai River sediments. The dash arrow line indicates decreasing mean size along the downstream.

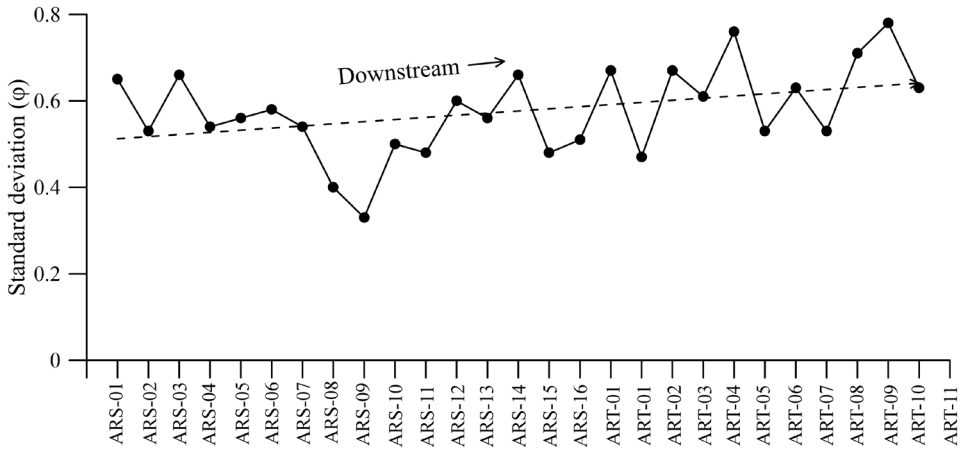

Fig. 4. Spatial distribution of sorting of the Atrai River sediments. The dash line indicates increasing sorting along the downstream.

Graphic Standard Deviation (SD)

The uniformity of grain size or sorting of clastic sediment is determined by

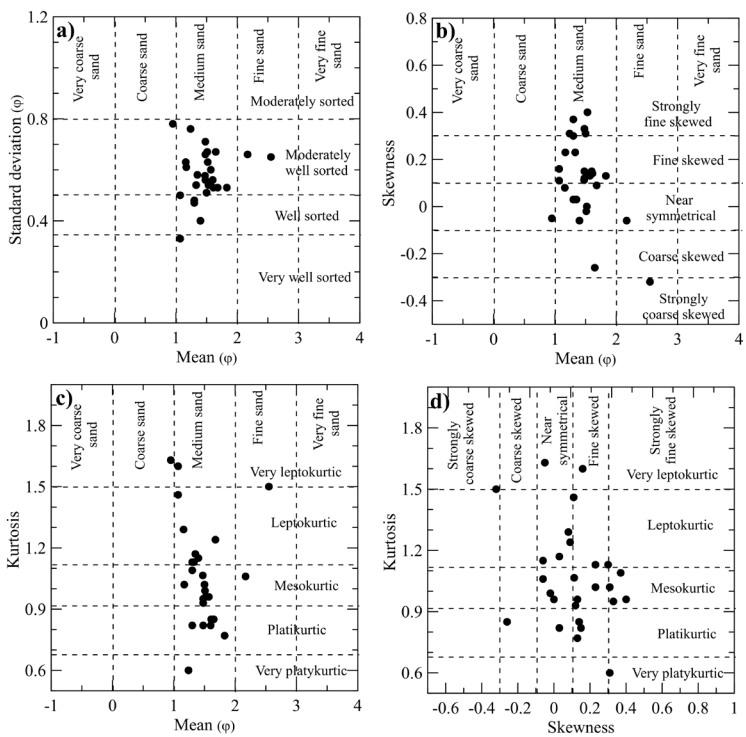

Fig. 5. Scatter plots of the textural parameters for the Atrai River sediments: **a**) mean vs. standard deviation; **b**) mean vs. skewness; **c**) mean vs. kurtosis and **d**) skewness vs. kurtosis.

the inclusive standard deviation. It clarifies to understand the hydrodynamics of sedimentary basin mechanism. The sorting results of the Atrai River sediments vary from 0.33φ to 0.78φ (Table 1; Fig. 5a), which demonstrates that the sediments are moderately well-sorted to well sorted. Moderately well sorting of sediments is attributed to regular winnowing practice of the depositing agents, probably due to the medium level of energy of the depositional media (BOGGS 2009). However, moderately well sorting of the sediments indicates uniform current flow prevailed during the deposition of the Atrai River sediments. The spatial distribution shows that the sorting of the Atrai River sediments increasing downstream (Fig. 4).

Graphic Skewness (SK)

Skewness measures the symmetry of grain size distribution. It indicates supremacy of coarse and fine-grained sediments in the cumulative frequency curves. The dominance of coarse grain sediments in the tail indicates negative skewness, whereas excess fine grain sediments in the tail indicate positive skewness (BOGGS 2009). The skewness of the studied sediments varies from -0.32 to 0.40 (Table 1; Fig. 5b, d) indicating coarse skewed to strongly fine-skewed nature of the Atrai River sediments. The fine skewed (~48%) character of sediments suggests excessive riverine input. About 78% of the samples are positively skewed (Table 1). The positive skewness of these sediments demonstrates the unidirectional channel transport or the deposition of sediments in low to medium level of energy environment (RAMANATHAN *et al*. 2009; HAKRO *et al*. 2021).

Graphic kurtosis (KG)

Graphic kurtosis estimates the proportion of sorting in the middle of the frequency curves, which represents sharpness of the frequency curves (Fig. 2). The kurtosis of the investigated Atrai River sediments varies between 0.60 and 1.63 (Table 1). Most samples show platykurtic to very leptokurtic with substantial dominancy of mesokurtic nature (Fig. 5c, d), which suggest a periodic variability of the sediment transporting agent.

Bivariate plots of statistical parameters

Cross-plots of textural parameter of clastic rocks or sediments provide important clues for understanding the nature of depositional setting and energy condition of the sediment transporting medium (FOLK & WARD 1957). The bivariate plots of the grain size parameters are also used to discriminate between fluvial, coastal, and aeolian depositional setting interpretation (FOLK & WARD 1957; FRIEDMAN 1967; PASSEGA 1964; SAHU 1964; STEWART 1958).

In mean vs. standard deviation bivariate plot (Fig. 6a), the Atrai River sediments are clustered at the half-way in the downward hook of the right-hand limb of "V" shaped trend proposed by FOLK & WARD (1957). In addition, the grain size range is

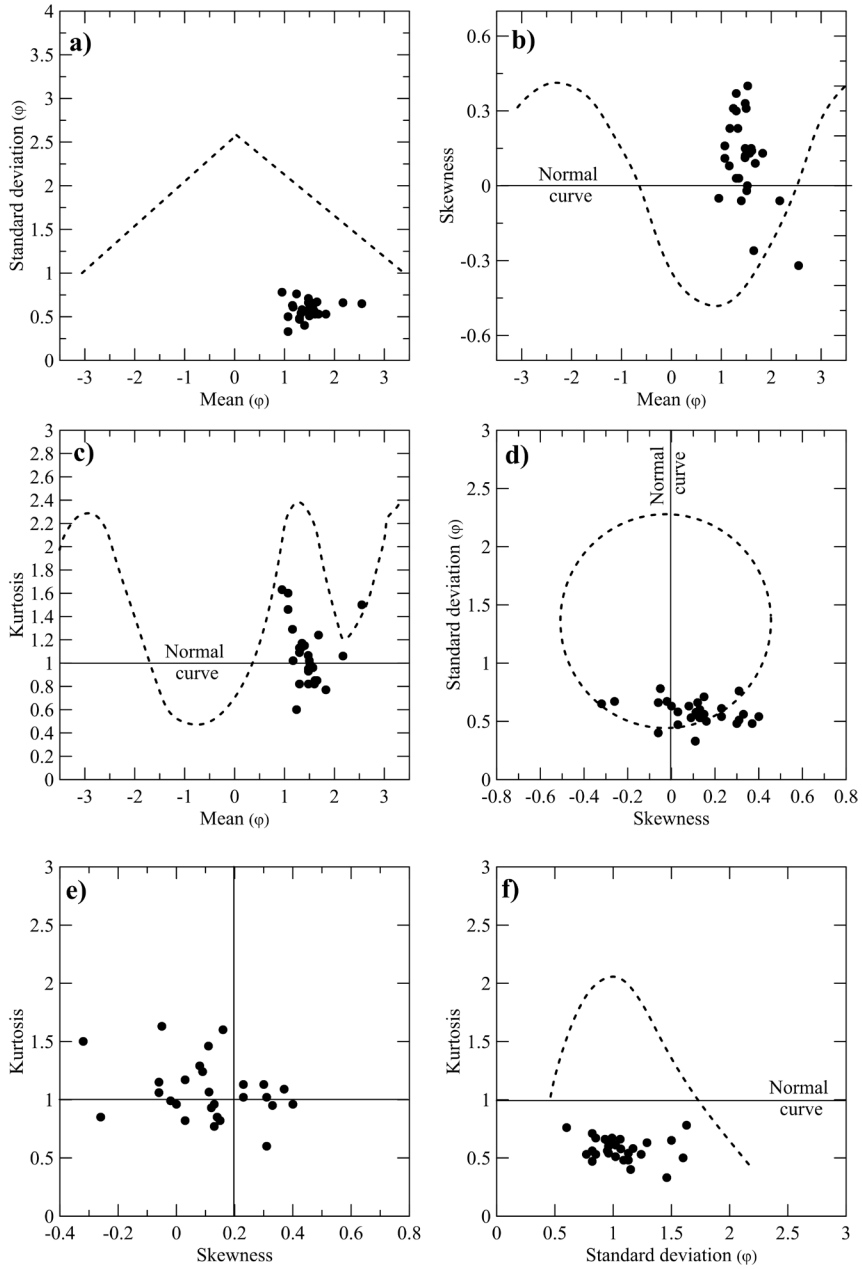

Fig. 6. Bivariate model plots for the Atrai River sediments (FOLK & WARD 1957): **a**) mean vs. standard deviation; **b**) mean vs. skewness; **c**) mean vs. kurtosis; **d**) skewness vs. standard deviation; **e**) skewness vs. kurtosis; **f**) standard deviation vs. kurtosis.

very smaller. These indicate unimodal nature of sand particles with better sorting. The well sorting of the investigated samples is also supported by this diagram, where FOLK & WARD (1957) proposed that the best sorting occurs with standard deviation between 0.4φ and 0.7φ. Textural parameters of siliciclastic sediments, especially the mean and sorting are controlled by hydraulics (FOLK & WARD 1957). In Fig. 6b, skewness is a very close function of grain size. Generally, pure modal fractions are near symmetrical, but with the mixing of two modes produce negative skewness if the finer mode is most abundant and positive skewness if the coarser mode is more abundant (FOLK & WARD 1957). However, sediments in the right-hand limb of the sinuous trend (Fig. 6b) indicate mixing of finer silt mode to the dominant fine sand mode. Whereas, scattering in the left-hand limb indicates mixing of coarser gravel mode to the dominant sand mode. In this diagram (Fig 6b), the investigated samples are scattered close to the right-hand trend and dominantly positive skewness (~78%). These suggest domination of sand mode with minor addition of silt mode in the Atrai River sediments and deposition took place under a medium energy setting (HAKRO *et al*. 2021).

The mean vs. kurtosis is highly complex and conceptual relationship between two sediment attributes (FOLK & WARD 1957). In this diagram (Fig. 6c), pure sand or gravel modes provides nearly normal curve with Kg = 1.0. Poor sorting results with addition of finer modes and scattered in the tail, whereas samples in the central part suggests better sorting (FOLK & WARD 1957). However, samples with Kg > 1 suggest leptokurtic, while Kg < 1 indicates platykurtic. On mean vs. kurtosis diagram (Fig. 6c) the studied sediments are scattered in nearly central part with little affinity toward the tail and kurtosis values are oscillating around 1. These results demonstrate that the Atrai River sediments are nearly pure sand modes with smaller mixing of finer modes and mesokurtic, leptokurtic and platykurtic, indicating poor to moderately well sorting.

In skewness vs. sorting plot the sediments dispersed in an almost circular trend (FOLK & WARD 1957). The mechanism for this dispersion may be either unimodal distribution in good sorting or an even blend of two modes. The dispersion of the investigated sediments indicates that 66% samples are clustered in the circular field and the remaining 33% samples are out of the field (Fig. 6d). This suggests the domination of unimodal nature of sediment with the mixing of another finer mode and moderately sorted. Skewness vs. kurtosis bivariate diagram indicates depositional modes (FOLK & WARD 1957). On skewness vs. kurtosis diagram (Fig. 6e) the data are dispersed almost in the center of the two attributes indicates unimodal sediments with the little affinity of another mode. The narrow range of skewness and kurtosis (Fig. 6e) reveals Atrai River sediments were being deposited in the effective sorting of the depositional environment. In standard deviation vs. kurtosis plot (Fig. 6f) the studied samples are dispersed below the normal curve, which represents uniform mode with moderately well sorting depositional setting.

Heavy mineral distribution

The heavy mineral composition of the Atrai River sediments are listed in Table 2 and also shown in Fig. 7. The heavy minerals of the studied sediments show the predominance of meta-stable heavy minerals following the order of garnet > epidote > sillimanite > kyanite > staurolite > apatite. The ultra-stable heavy mineral suite (ZTR-zircon, tourmaline, rutile) is followed by tourmaline > rutile > zircon. The unstable hornblende exceeds the pyroxene. Significant concentrations of opaque minerals (10.47%) have been noticed in the investigated sediments. The microscopic characteristics of the heavy minerals are discussed in the following section:

Table 2. Heavy mineral concentrations (%) from the bar sediments of upper reaches of the Atrai River.

Sample No.	Gar	Epi	Sill	Ky	Sta	Tou	Hor	Ru	Zir	Apa	Py	Opa	Ot
ARS-01	29.14	2.36	11.29	5.90	1.40	9.42	7.53	5.66	1.87	6.12	8.47	8.20	2.64
ARS-03	30.00	4.73	9.96	5.68	6.16	6.63	4.26	5.21	2.38	3.78	7.11	8.33	5.77
ARS-05	19.84	3.23	23.39	7.25	5.64	5.64	11.29	0.80	0.20	2.43	4.84	10.64	4.81
ARS-07	20.20	3.66	15.12	4.39	2.45	7.66	8.75	1.68	1.13	2.25	4.39	8.51	19.81
ARS-10	28.83	5.15	16.03	8.86	5.39	7.16	4.15	1.56	1.56	4.35	3.65	8.30	5.01
ARS-11	22.62	3.42	14.37	9.35	5.24	6.97	5.46	2.05	1.15	2.52	4.05	8.96	13.84
ARS-14	23.11	4.35	14.81	11.34	9.58	4.35	6.11	3.49	1.53	3.49	3.49	9.35	5.00
ARS-16	27.93	3.79	14.41	8.34	7.58	3.03	3.79	1.52	1.27	1.52	3.03	8.79	15.00
ART-01	9.94	12.28	9.94	8.77	11.11	6.43	5.26	1.20	0.90	1.34	5.85	12.30	14.68
ART-02	13.82	14.47	8.55	9.21	3.29	2.63	3.95	4.61	1.20	2.63	3.29	9.60	22.75
ART-03	10.65	15.38	4.73	13.61	6.51	4.14	4.14	1.78	1.53	1.18	4.14	12.23	19.98
ART-04	14.71	11.76	12.35	5.29	7.06	10.59	7.06	1.76	0.80	0.59	1.18	10.43	16.42
ART-05	16.48	18.13	6.59	10.44	3.85	7.14	4.40	0.55	1.10	1.10	1.10	13.21	15.91
ART-06	16.95	18.64	2.82	10.73	5.08	7.34	4.52	0.56	1.60	1.13	1.69	12.45	16.49
ART-07	14.77	17.61	6.82	10.23	4.55	2.84	6.25	1.70	2.00	0.50	0.57	14.43	17.73
ART-08	23.35	24.67	3.96	5.73	6.17	4.85	3.08	1.32	0.70	1.32	2.20	9.37	13.28
ART-09	22.50	13.00	10.00	6.00	5.00	3.50	4.50	1.00	1.43	0.50	1.50	12.33	18.74
ART-10	20.86	15.51	9.09	6.42	4.28	3.74	2.67	1.07	1.60	1.07	1.60	10.10	21.99
ART-11	23.72	16.28	6.98	8.84	4.19	3.72	2.33	1.40	1.00	0.47	1.86	11.44	17.77
Average	**20.50**	**10.97**	**10.59**	**8.23**	**5.50**	**5.67**	**5.24**	**2.05**	**1.31**	**2.02**	**3.37**	**10.47**	**14.09**

Gar-garnet, Epi-epidote, Sill-sillimanite, Ky-kyanite, Sta-staurolite, Hor-Hornblende, Tou-tourmaline, Ru-rutile, Zir-zircon, Apa-apatite, Py-pyroxene, Opa-opaque, Ot-others.

Garnet: Generally garnet grains are colorless, but in some cases pale pinkish grains are also recognized (Fig. 8a, b). It shows very high relief together with isotropic nature. The average concentration of garnet is 20.50 %, where the highest value ranged up to 30% in the investigated samples (Table 2).

Epidote: Epidote is identified by its high relief, characteristic yellowish green, pale green

or pale brown color, strong pleochroism, one directional perfect cleavage, parallel extinction as well as irregular morphology (Fig. 8m). The average concentration of epidote is about 10.97% in the Atrai River bar sediments.

Staurolite: It is identified by its high relief, yellowish brown or golden yellow color (Fig. 8j), and parallel extinction. The concentration of staurolite varies from 1.40% to 11.11% with an average value of 5.50% in the Atrai River bar sediments.

Kyanite: Kyanite is typically colorless. It is characterized by bladed or prismatic habit, step-like feature (Fig. 8h, i) together with the combination of high relief, perfect cleavage and oblique extinction. The average concentration of kyanite is about 8.23% in the studied sediments.

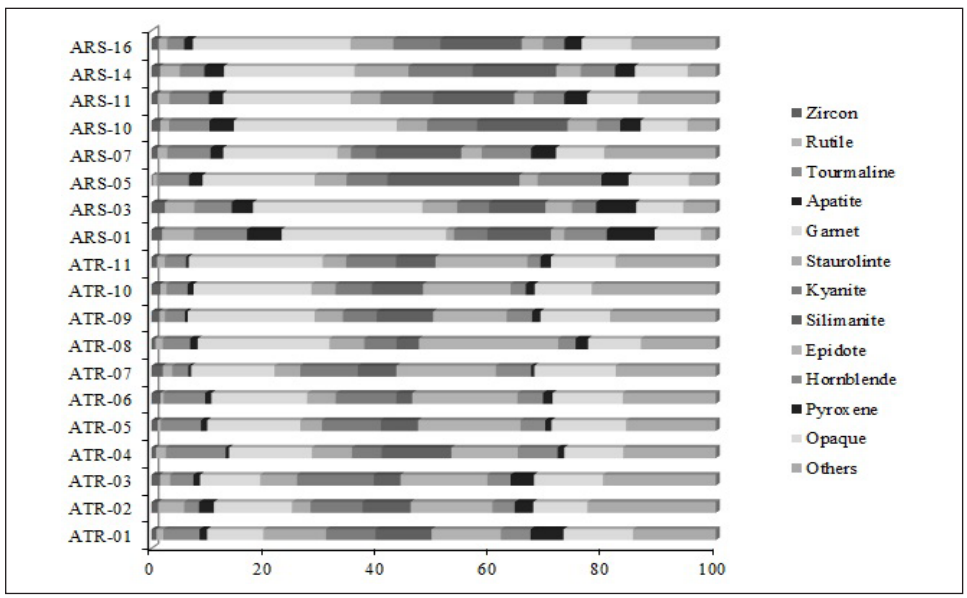

Fig. 7. Heavy mineral concentration (%) of the bar sediments from the upper reaches of the Atrai River.

Sillimanite: Sillimanite is colorless to less commonly pale yellow and brown (Fig. 8k, l). It is identified by its prismatic or fine fibrous crystal habit, high relief, perfect cleavage, parallel extinction and moderate or fairly distinctive interference colors. The concentration of sillimanite ranges 2.82-23.39% with an average concentration of about 10.59%.

Tourmaline: Tourmaline shows variable color generally golden brown or pale yellowish brown (Fig. 8f, g) and strongly dichroic. It is identified by its moderate relief, highly variable morphology (usually prismatic and hexagonal form), marked pleochroism and lack of cleavages. It is a unique mineral that shows light absorption

property with rotating stage under plane polarized light. The concentration of tourmaline in the samples varies from 2.63% to 10.59% with an average value of 5.67%.

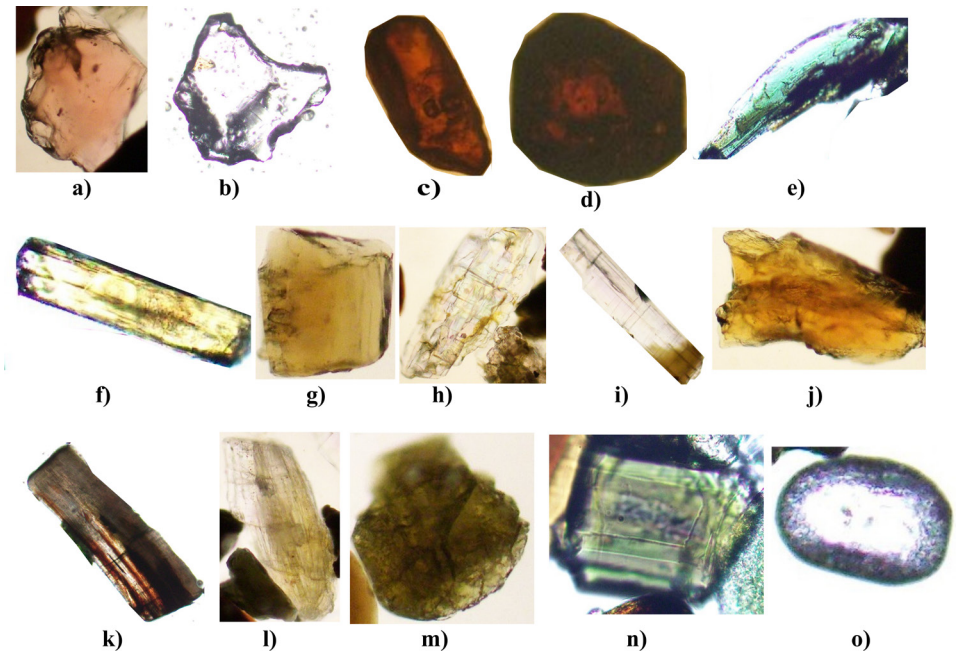

Fig. 8. Photomicrograph of heavy minerals under plane polarized light (10x): **a-b**) garnet; **c-d**) rutile; **e**) hornblende; **f-g**) tourmaline; **h-i**) kyanite; **j**) staurolite; **k-l)** sillimanite; **m**) epidote; **n-o**) zircon.

Rutile: Rutile is identified by its very high relief, deep red, red-brown or yellow brown color (Fig. 8c, d), weak pleochroism, parallel extinction and extreme birefringence. The concentration of rutile in the Atrai River bar sands varies from 0.55% to 5.66% with an average value of 2.05%.

Zircon: Zircon is colorless to yellowish brown color and occurred as sharp hexagonal, euhedral to subhedral crystals through prismatic fragments and rounded to well-rounded forms (Fig. 8n, o). It is identified by its extreme high relief, weak pleochroism, parallel extinction and strong birefringence. Some grains are characterized by inclusions and thick black halo surrounding the grains (Fig. 8n, o). It is found with an average value of 1.31%.

Hornblende: It is characterized by prismatic, elongated and columnar morphology, bluish green or brownish green color (Fig. 8e) moderate to high relief, perfect cleavage and moderate to strong pleochroism. It is observed in all samples with an average

concentration of about 5.24%.

Pyroxene: It appears in colorless with pale green tinge, various shades of green, brown, yellowish brown, pale reddish-brown color and fairly high relief. The average concentration of pyroxene is 3.37% and maximum value ranged up to 8.47% (Table 2).

Apatite: Apatite is colorless and nonpleochroic and is identified by its moderately high relief, oval shaped morphology, parallel extinction and weak birefringence. The average concentration of apatite is about 2.02%.

Opaque minerals: Opaque minerals occur as totally black under plane and cross polarizing microscope. Different types of iron oxides, like magnetite, ilmenite, pyrite, hematite etc., may present as opaque minerals. The average concentration of opaque minerals in studied sediments is 10.47%.

Discussion

Depositional processes

The textural behavior, like medium grain (average mean size 1.47φ), moderately well sorting (0.58φ) and positive skewness (Fig. 5b, 6b) support a river–link deposit (FRIEDMAN 1979). The dominance of positive skewness and mesokurtic to leptokurtic nature of sediments suggests unimodal and moderately well sorting deposition under a medium energy setting.

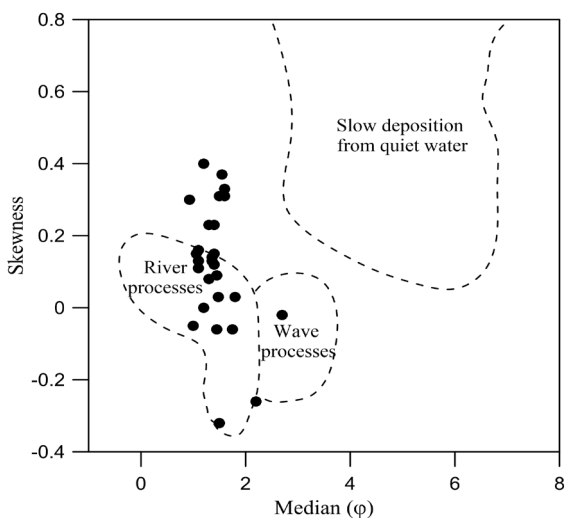

Fig. 9. Bivariate plot of skewness vs. median discriminates the depositional processes of the Atrai River sediments (fields are after STEWART 1958).

Though few samples show negative skewness and platykurtic nature (Fig. 5b, c), which are due to continuous addition of finer modes with the dominant sand modes. STEWART (1958) used median vs. skewness to discriminate depositional processes of river, wave and quite water slow depositional (Fig. 9) environment. According to this diagram most of the investigated samples fall within the river field and some samples are dispersed between the river and quite water slow deposition fields. These results demonstrate that the Atrai River sediments were deposited mainly in a fluvial environment with medium energy condition. The bivariate plot of mean grain size against sorting is a reliable means of reconstructing fluvial and estuarine environments. MAKHLOUF *et al*. (1991) proposed this model to separate zones of high and low energy in fluvial and estuarine environments. In this study, the corresponding plot (Fig. 10) shows that all the sediment samples are dispersed well within the fluvial zone characterized by stream episodes.

KANHAIYA *et al*. (2017) introduced a bivariate plot of mean grain size against sorting of the Ganga river sediments to discriminate between channel and Floodplain deposits in the fluvial setting. The activity diagram (Fig.11) demonstrates that the Atrai

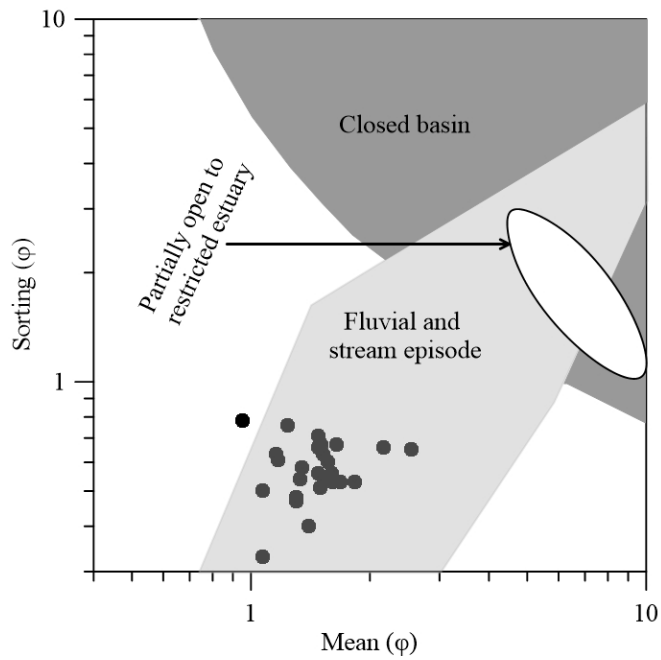

Fig. 10. Bivariate plot of mean grain size against sorting for the Atrai River sediments (fields are after MAKHLOUF *et al*. 1991).

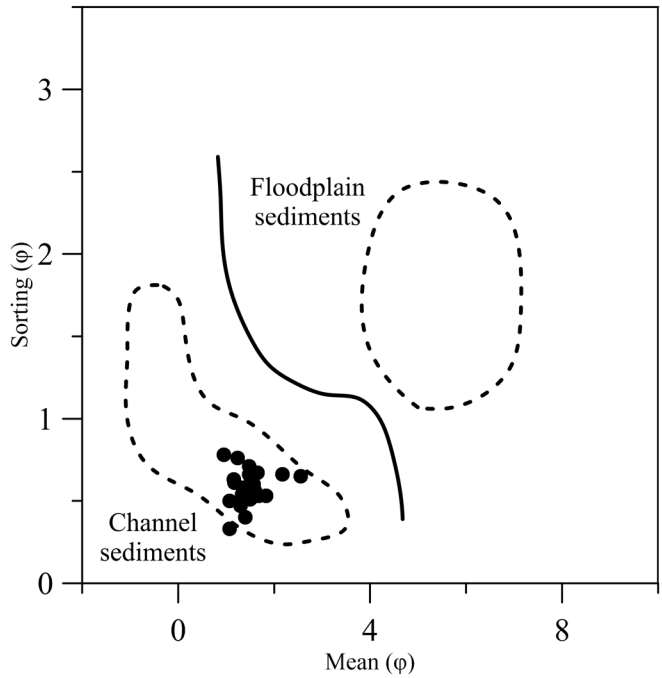

Fig. 11. Bivariate plot of mean grain size against sorting (after KANHAIYA *et al*. 2017) for the Atrai river sediments. The solid line separates the channel and floodplain deposits in the activity diagram.

River sediments are discriminated into channel deposits. Grain size parameters and the plots of CM (C = 1percentile; M = median) patterns helps to distinguish between the sediments of different depositional settings of fluvial deposits (PASSEGA & BYRAMJEE 1969). In this study an attempt has been made to identify the modes of sediment deposition in the upper reaches of the Atrai River bar sediments by CM pattern (Fig. 12). Relation between C and M is the effect of sorting by bottom turbulence. The investigated sediments show that samples from the upper most part the Atrai River are scattered in the OP segment of the CM diagram (Fig. 12), which suggest rolling and suspension mode of sediment deposition. On the other hand, the samples from the relatively downstream part are dispersed in the PQ segment, indicate the sediments were transported by rolling and suspension (Fig. 12) before being deposited.

Sorting values vary systematically with the mean size in the bedload and the suspended load sediments. SING *et al*. (2007) proposed a model of skewness vs. standard deviation for the bedload and the suspended load sediments. The application of this diagram (Fig. 13) in the investigated samples suggest that the Atrai River sediments were transported dominantly by bedload mechanism.

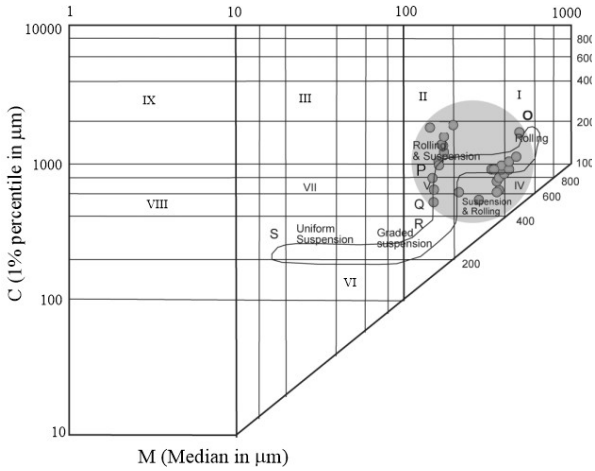

Fig. 12. C-M diagram showing transport mechanism of the Atrai River sediments (fields are after PASSEGA & BYRAMJEE 1969).

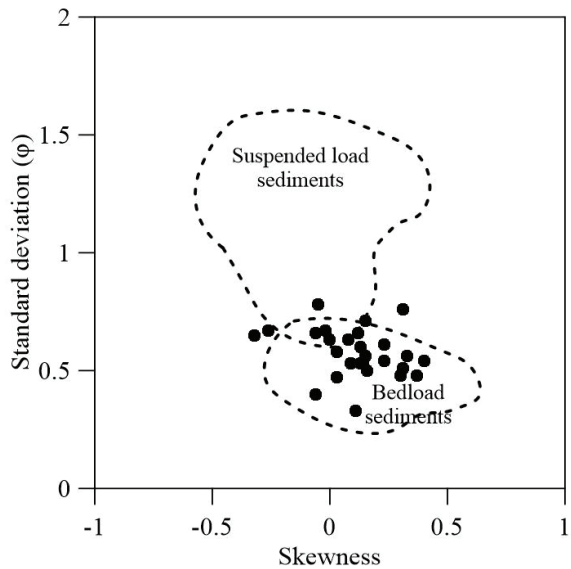

Fig. 13. Bivariate plot of skewness vs. standard deviation (after SING *et al*. 2007) to discriminate the modes of sediment transport of the Atrai River sediments.

Provenance

Heavy mineral suites provide important information of source rock complexes in the provenance. The mineralogical maturity of heavy mineral assemblage is defined by ZTR (Zircon-Tourmaline-Rutile) index (Fig. 14a). The ZTR values of the studied

samples range from 6.38% to 18.46% with an average value of 10.06% (Table 3). The low ZTR value indicates the sediments are mineralogically immature. The shapes of the mineral grains are dominantly elongated and subhedral to anhedral, which indicates short transportation of sediments and were deposited close to the sources. The Atrai River sediments consist of higher concentrations of meta-stable heavy minerals (garnet, epidote, kyanite and staurolite) rather than the stable ZTR minerals (Fig. 14b). Based on the result, the Atrai River bar sediments comprise the following heavy mineral assemblages: i. garnet, epidote, kyanite, sillimanite and staurolite; ii. zircon, tourmaline, rutile, apatite and hornblende; and iii. pyroxene and opaque minerals.

A metamorphic provenance is indicated by the presence of heavy mineral suite of garnet, epidote, kyanite, staurolite and sillimanite. The possible source of garnet is mica-schist and gneiss complexes and related metamorphic rocks (FAUPL *et. al*. 1988). A low to medium grade metamorphic source area is indicated by the presence of epidote. Sillimanite occurs in high-temperature metamorphic rocks which containing clay (biotite-horfels). Kyanite is usually found in high pressure metamorphic rocks (such as schists and gneisses). Medium-grade pelitic metamorphic rock is suggested by the occurrence of staurolite (UDDIN & LUNDBERG 1998). However, a metamorphic provenance is also suggested by the occurrence of pink and pale brown verities of tourmaline (BLATT *et al.* 1980). In addition, the existence of high pressure/low temperature metamorphic rocks is also indicated by presence of hornblende. The abundances of meta-stable heavy minerals were also reported from the Jamuan and Meghna River sediments (ABEDEN *et al*. 2018; RAHMAN *et al*. 2022) and Miocene sediments of the Bengal Basin (DINA *et al*. 2016; UDDIN & LUNDBERG 1998) and also from the Bengal and Nicobor deep-sea fans (THOMPSON 1974).

An acid igneous source rock complex is suggested by the presence of heavy mineral suite of zircon, tourmaline, rutile, apatite and hornblende. The presence of zircon indicates the source as intrusive acid igneous rock (AHMED & ISLAM 2001). Tourmaline is a characteristics mineral of granitic pegmatites. Larger crystal of rutile is a common accessory in pegmatites. The occurrences of apatite and hornblende are suggestive of acid igneous and high grade metamorphic provenance (THOMPSON 1974). However, the presence of apatite believed to have derived from biotite-rich source rocks (FAUPL 1998).

A basic igneous provenance is indicated by the presence of pyroxene and opaque minerals. Pyroxene is a common mineral in basic rocks (THOMPSON 1974),

like gabbro and basalt. However, significant concentrations of opaque minerals (average 10.47%) also indicate a basic source complex. The rounded to sub-rounded rutile and zircon (Fig. 8c, o) are probably recycled from the sedimentary and/or meta-sedimentary provenance.

This study examined several heavy mineral indices (Table 3) to evaluate the provenance and sediment maturity of the Atrai River sediments. Generally, similar values of ZTR, ATi, GZi and RZi indicate the same source area (MENG *et al*. 2016; SUN *et al*. 2020). The investigated results reveal a wide range of variations of ZTR (6.38% to 18.46%), ATi (5.28% to 50%), GZi (87.44% to 99.00%) and RZi (25.93% to 80.00%) values, which suggest that the terrestrial inputs for the Atrai River came from the different source area. In addition, the binary plots of ATi, GZi, RZi ratios and stability index showed apparent variations to the ZTR index and poor correlation (Fig. 15). The linear relationships of ATi and RZi with ZTR (Fig. 15a, c) show poorly positive correlation, which apparently suggest that apatite, zircon, rutile and tourmaline almost came from the similar sources. On the other hand, Gzi shows no obvious correlation with ZTR (Fig. 15b) and stability index shows poor negative correlation with ZTR (Fig. 15d), indicating Atrai River detritus were originated from different sources. However, the negative poor correlation of the stability index (Fig. 15d) suggests that the Atrai River sediments are immature in nature.

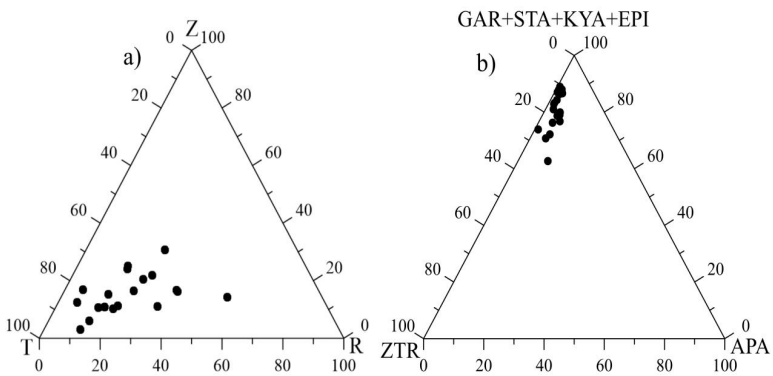

Fig. 14. Triangular plot of: **a**) ZTR index and **b**) (GAR+STA+KYA+EPI) – ZTR-APA for the upper Atrai River bar sediments (Z- zircon, T-tourmaline, R-rutile, G-garnet, Epi-epidote, Ky-kyanite, Sta-Staurolite, APA- apatite).

The Atrai River is originated from the northeast Himalaya and the catchment area comprises Higher Himalaya, Lesser Himalaya and Sub-Himalayan Ranges.

Table 3. Results of the heavy mineral indices of the of the Atrai River bar sediments (expressed in %).

Sample No.	ZTR	ATi	RZi	GZi
ARS-01	9.73	17.25	57.14	91.70
ARS-03	9.34	50.00	79.35	92.01
ARS-05	8.49	22.18	53.78	87.44
ARS-07	14.68	5.28	68.75	94.84
ARS-10	10.13	13.35	33.33	93.74
ARS-11	10.85	13.34	25.93	91.37
ARS-14	7.64	14.97	45.95	88.07
ARS-16	7.58	21.39	65.35	97.09
ART-01	6.76	12.50	41.15	94.02
ART-02	7.13	22.25	40.07	92.88
ART-03	6.91	11.22	58.33	95.95
ART-04	18.46	39.38	75.17	93.97
ART-05	15.51	36.31	68.64	92.65
ART-06	7.43	30.11	80.00	99.00
ART-07	11.44	22.70	59.79	94.70
ART-08	11.21	37.79	50.00	94.87
ART-09	11.17	26.55	64.06	95.16
ART-10	10.34	44.52	69.52	93.79
ART-11	6.38	33.41	54.48	95.65
Average	10.06	24.97	57.41	93.63

ZTR=100*(zircon+tourmaline+tourmaline)/total non-opaque minerals; ATi=(100*apatite/(apatite+tourmaline)); RZi=(100*rutile/(rutile+zircon)); GZi=(100*garnet/(garnet+zircon))

Based on petrological results of high-grade metamorphic and granitoid rocks comprise the Higher Himalaya (YOKOYAMA *et al*. 1990). The Lesser Himalaya crystalline basement is built up of low to medium grade rocks. Kyanite is a typical marker of the Higher Himalaya crystalline rocks, but is also found locally in Lesser Himalaya (PECHER 1989). The relative abundance of various aluminous silicates and epidote indicate orogenic input from low- to high-grade metamorphic rocks (UDDIN & LUNDBERG 1998). The Higher and Lesser Himalaya also comprise basic igneous rocks. The Lesser Himalaya contains sedimentary and meta-sedimentary rock complexes. The Sub-Himalayan Ranges consist of Neogene molasse type sediments including Siwaliks (KUNDU *et al*. 2016). Rounded and sub-rounded varieties of zircon and rutile indicate that they were probably recycled from sedimentary and meta-sedimentary sources.

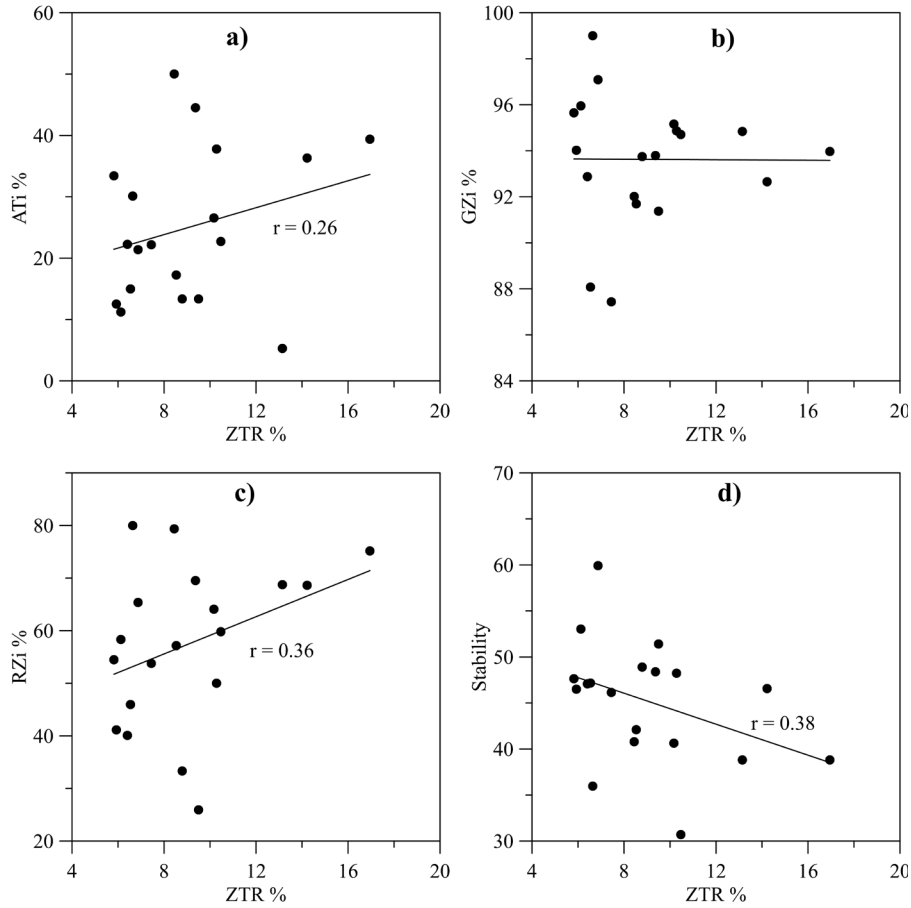

Fig. 15. Binary plot of heavy mineral stability indices (ZTR and stability indices) and heavy mineral ratios (ATi, GZi, and RZi) showing spatial variations of the Atrai River sediments (after MENG *et al*. 2016).

Conclusions

This study summarizes the following conclusions:

1. The upper reaches of the Atrai River sediments are medium grained (1.47φ), moderately well sorted (0.58φ), mesokurtic to leptokurtic in nature and dominantly positively skewed (~78%). All of these parameters are suggestive of excessive riverine input.
2. The bivariate diagrams of the textural parameters (mean vs. sorting, median vs. sorting) indicates the studied sediments were deposited in the channel floor under medium level of energy condition.

3. The CM diagram and bivariate plot of skewness vs. sorting indicate the sediments were deposited under rolling and suspension processes under bedload mechanism.

4. The heavy mineral suits suggests that the Atrai River sediments are mineralogically immature and were deposited close to the sources.

5. The heavy mineral concentrations of the Atrai River sediments reflect a variety of source rock complexes exist in the provenance. A low- to high-grade metamorphic source terrain is characterized by widespread distribution of the heavy mineral suite of garnet, epidote, kyanite, staurolite and sillimanite. Acid igneous provenance is reflected from the heavy mineral suite of zircon, rutile, tourmaline, apatite and hornblende. Basic igneous provenance is indicated by the presence of pyroxene and opaque minerals. Sedimentary or meta-sedimentary provenance is suggested by rounded to sub-rounded zircon and rutile.

6. The investigated results suggest that the sediments were derived from the high-grade and crystalline Higher Himalaya, low- to medium-grade rocks in the Lesser Himalaya and the Neogene molasses exposed in the Sub-Himalayan Ranges of the southeastern Himalayan syntaxes.

Acknowledgement

The authors are grateful to the Faculty of the Mathematical and Physical Sciences, Jahangirnagar University for supporting the financial grants for this research work.

References

Abeden, M.J., Rahman, M.J.J., Sayem, A.S.M. & Abdullah, R., 2018, Heavy mineral distribution in sand deposits from the lower reaches of the Jamuna River, Bangladesh; *Bangladesh Geoscience Journal*, **24**, 1–15.

Ahmed, S.S. & Islam, M.B., 2001, Economic minerals in the beach sands of the southeastern Bangladesh; In: Rajamanickam, G.V. (ed.), *Hand book of Placer Mineral Deposits*, New Academic Publishers, 280-294.

Ali, S., Alam, M.S., Ahmed, S.S., Zaman, M. N., Hossain, I. & Biswas, P.K., 2019, Geochemical characteristics of Recent sediments of channel bar of the Ganges (Padma) River, Bangladesh; *Bangladesh Geoscience Journal*, **25**, 23-46.

Blatt, H., Middleton, G.D. & Murray, R., 1980, *Origin of sedimentary rocks*; 2nd edition, Prentice-Hall, New Jersey, 782p.

Boggs, S., 2001, *Principles of sedimentology and stratigraphy*; 3rd ed., Prentice Hall, New Jersey, 726p.

Boggs, S., 2009, *Petrology of sedimentary rocks*; Cambridge University Press, 600p.

Dina N.T., Rahman, M.J.J., Hossain, M.S. & Sayem, A.S.M., 2016, Provenance of the Neogene succession in the Bandarban structure, south-east Bengal Basin, Bangladesh: Insights from perography and petrofacies; *Himalayan Geol.*, **32**, 141-152.

FAUPL, P., PAVLOPOULOS, A. & MIGIROS, G., 1998, On the provenance of flysch deposits in theExternal Hellenides of mainland Greece: results from heavy mineral studies; *Geol. Mag*., **135**, 421-442.

FOLK, R.L. & WARD, W.C., 1957, Brazos River bar: A study in the significance of grain size parameters; *J. Sedi. Petrol*., **27**, 3-26.

FOLK, R.L., 1968, *Petrology of sedimentary rocks*; *Hemphill publishing company*, Austin, Texas, 170p.

FRIEDMAN, G.M., 1961, Distinction between dune, beach and river sands from their textural characteristics; *J. Sedi. Petrol*., **31**, 514-529.

FRIEDMAN, G.M., 1967, Dynamic processes and statistical parameters compared for grain frequency distribution of beach and river sands; *J. Sedi. Petrol.*, **37**, 327-354.

FRIEDMAN, G.M., 1979, Differences in size distributions of populations of particles among sands of various origins; *Sedimentology*, **26**, 3-32.

HAKRO, A. A., XIAO, W., MASTOI, A. S., YAN, Z., SAMTIO, M. S. & RAJPER, R. H., 2021, Grain Size analysis of the Oligocene Nari Formation sandstone in the Laki Range, southern Indus Basin, Pakistan: Implications for depositional setting; *Geoloigcal. J*., **56**, 5440-5451.

HOSSAIN, H. M. Z., 2019, Major, trace, and REE geochemistry of the Meghna River sediments, Bangladesh: Constraints on weathering and provenance; *Geol. J.*, **55**, 3321–3343.

KANHAIYA, S., SINGH, B.P., TRIPATHI, M., SAHU, S. & TIWARI, V., 2017, Lithofacies and Particle size characteristics of late Quaternary floodplain deposits along the middle reaches of the Ganga river, central Ganga plain, India; *Geomorphology*, **284**, 220-228.

KUNDU, A., MATIN, A. & ERIKSSON, P.G., 2016, Petrography and geochemistry of the Middle Siwalik sandstones (Tertiary) in understanding the provenance of sub-Himalayan sediments in the Lish River Valley, West Bengal India; *Arabian J. Geosci.,* **9**(2), 162.

MAKHLOUF, I.M., TURNER, B.R. & ABED, A.M., 1991, Depositional facies and environments in the Permian Umm Irna formation, Dead Sea area, *Jordan; Sedi. Geol*., **73**, 117-139.

MANGE, M.A. & MAURER, H.F.W., 1992, *Heavy minerals in color*; Chapman and Hall, London, 133p.

MASON, C.C. & FOLK, R.L., 1958, Differentiation of beach, dune and aeolian flat environments by grain size analysis, Mustang Island, Texas; *J. Sedi. petrol,* **28**, 211-226.

MENG, Y., DONG, H., CONG, Y., XU, Z. & CAO, H., 2016, The early-stage evolution of the NeoTethys Ocean: evidence from granitoids in the middle Gangdese batholith, southernTibet; *J. Geodynamics*, **94**,34-49.

PASSEGA, R., 1957; Texture as characteristic of clastic deposition; *Am. Assoc. Geologists Bull*., **41**, 1952-1987.

PASSEGA, R., 1964, Grain size representation by CM patterns as a geological tool; *J. Sedi. Petrol*., **34**, 830-847.

PASSEGA, R. & BYRAMJEE, R., 1969, Grain-size image of clastic deposits; *Sedimentology*, **13**, 23325.

PECHER , A., 1989, The metamorphism in the Central Himalaya; *J. Metamorphic Geol*., **7**(1), 31-41.

RAHMAN, M.A., DAS, S.C., POWNCEBY, M.I., TARDIO, J., ALAM, M.S. & ZAMAN, M.N., 2020, Geochemistry of recent Brahmaputra River sediments: provenance, tectonics, source area weatehring and depositional environment; *Minerals,* **10**, 813.

RAHMAN, M.J.J, XIAO, W., HOSSAIN, S.M., YEASMIN, R., SAYEM, A.S.M., AO, S., YANG, L. & ABDULLAH, R., 2020, Geochemistry and detrital zircon U-Pb dating of Pliocene-Pleistocene sandstones of the Chittagong Fold Belt (Bangladesh): Implications for provenance; *Gondwana Research*., **78**, 278-290.

RAHMAN, M.J.J., POWNCEBY, M.I. & RANA, M.S., 2022, Distribution and charaterization of heavy minerals in Meghna river sand deposits, Bangladesh; *Ore Geol. Rev.*, **143**, 104773.

RAHMAN, M.M., HASAN, M.F., HASAN, A.S.M.M., ALAM, M.S., BISWAS, P.K. & ZAMAN, M.N., 2021, Chemical weathering, provenance and tectonic setting inferred from recently deposited sediments of Dharla River, Bangladesh; *J. Sedi. Envir.*, **6**, 73-91.

RAMANATHAN, A. L., RAJKUMAR, K., MAJUMDAR, J., SINGH, G., BEHERA, P. N., SANTRA, S. C. & CHIDAMBARAM, S., 2009, Textural characteristics of the surface sediments of a tropical mangrove Sundarban ecosystem India; *Indian Journal of Geo-Marine Sciences*, **38**, 397-403.

SAHU, B.K., 1964, Depositional Mechanisms from the Size Analysis of Clastic Sediments; *J. Sedi. Petrol.*, **34**, 73-83.

SAYEM, A.S.M. & RAHMAN, M.J.J., 2012, Sandstone petrology of the Surma Group succession exposed in the Sitapahar Anticline, Bengal Basin, Bangladesh; *Bangladesh Geoscience Journal.* **12**, 15-31.

SINGH, M., SINGH, I.B. & MÜLLER, G., 2007, Sediment characteristics and transportation dynamics of the Ganga River; *Geomorphology*, **86**, 144-175.

STEWART , H.B., 1958, Sedimentary reflections of depositional environment in San Miguellagoon, Baja California, Mexico; *AAPG Bull*., **42**, 2567-2618.

SUN, Z., ZHU, H., XU, C., YANG, X. & DU, X., 2020, Reconstructing provenance interaction of multiple sediment sources in continental down-warped lacustrine basins: An example from the Bodong area, Bohai Bay Basin, China; *Marine and Petroleum Geol*., **113**,104142.

THOMPSON, R.W., 1974, Mineralogy of sands from the Bengal and Nicobar Fans, Sites 218 and 211, Eastern Indian Ocean; In: VON DER BORCH, C.C., SCLATER, J.G. (eds), *Initial Reports of the 788 Deep Sea Drilling Project*, 22, 711–713; United States Government Printing Office, Washington, DC.

UDDEN, J.A., 1914, The Mechanical composition of clastic sediments; *Geo. Soc. Amer. Bull.,* **110**, 497-511.

UDDIN, A. & LUNDBERG, N., 1998, Unroofing history of the eastern Himalaya and the Indo–Burman ranges: heavy mineral study of Cenozoic sediments from the Bengal Basin, Bangladesh; *J. Sedi. Res*., **68**, 465–472.

YOKOYAMA, K., AMANO, K., TAIRA, A. & SAITO, Y., 1990, Mineralogy of silts from the Bengal fan; In:COCHRAN, J.R., STOW, D.A.V., *Proceedings of the Ocean Drilling Program, Scientific Results*, **116**; College Station, TX (Ocean Drilling Program) 59-73.

Accepted 15 May, 2023

বাংলাদেশের উত্তর-পশ্চিমে আত্রাই নদীর উজানের চর পললের বুনন ও ভারী খনিজের বৈশিষ্ট্য

আবু সাদাত মো: সায়েম, খন্দ. ফারজানা জোহা, মো: রোকনুজ্জামান,
জয়নুল আবেদীন ও জাহিদুল বারী

সারসংক্ষেপ

আত্রাই নদীর উৎপত্তি হিমালয়ের দক্ষিণ-পূর্বে এবং এটি বঙ্গীয় অববাহিকায় প্রমত্তা ব্রহ্মপুত্র নদীর অন্যতম প্রধান উপনদী হিসেবে বিবেচিত হয়। এই প্রবন্ধটিতে আত্রাই নদীর উজানের চরে জমাকৃত পললের বুনন ও ভারী খনিজের বৈশিষ্ট্য উপস্থাপন করা হয়েছে। পলল বুনন বৈশিষ্ট্যগুলি নির্দেশ করে যে আত্রাই নদীর পলল মাঝারি থেকে সূক্ষ্ম দানাদার (১.৪৭φ), মাঝারি-ভালভাবে সাজানো (০.৫৮φ), ধনাত্মক স্কিউড (৭৮%) এবং মেসোকার্টিক থেকে লেপ্টোকারটিক প্রকৃতির। বিভিন্ন দ্বিমুখী চিত্রগুলো নির্দেশ করে যে বিশ্লেষণ করা পললসমূহ একটি মাঝারি শক্তির স্রোতের অধীনে নদীর তলদেশে জমা হয়েছিল। প্রাপ্ত ফলাফল আরও নির্দেশ করে যে পললসমূহ বেশিরভাগ বেডলোড পলল এবং রোলিং এবং সাসপেনশন প্রক্রিয়া দ্বারা জমা হয়েছিল। ভারী খনিজ বিশ্লেষণ স্থিতিশীল ভারী খনিজগুলির (জিরকন, রুটাইল এবং ট্যুরমালাইন) তুলনায় স্বল্প-সুস্থিত ভারী খনিজগুলির (গারনেট, এপিডোট, স্টাউরোলাইট, কায়ানাইট এবং সিলিমানাইট) প্রাধান্যকে প্রতিফলিত করে। গারনেট, এপিডোট, কায়ানাইট, স্টোরোলাইট এবং সিলিমেনাইটের ভারী খনিজ সংঘটন দ্বারা একটি নিম্ন থেকে উচ্চ-গ্রেডের রূপান্তরিত শিলা উৎস ভূখণ্ডের নির্দেশ দেয়। অম্ল আগ্নেয় উৎস জিরকন, রুটাইল, ট্যুরমালাইন, এপাটাইট এবং হর্নব্লেন্ডের সংঘটন দ্বারা প্রতিফলিত হয়। পাইরক্সিন এবং অস্বচ্ছ খনিজগুলির উপস্থিতি দ্বারা একটি ক্ষারীয় আগ্নেয় শিলার উৎসস্থল নির্দেশিত হয়। গোলাকার ও উপ-গোলাকার জিরকন এবং রুটাইলের খনিজগুলি পাললিক এবং স্বল্প রূপান্তরিত-পাললিক উৎসের নির্দেশ করে। সুতরাং, ইহা প্রতীয়মান হয় যে আত্রাই নদীর পলিগুলি মিশ্র উৎস, সম্ভবত উচ্চ হিমালয়ের পূর্ব অংশ, স্বল্প উচ্চ হিমালয় এবং দক্ষিণ-পূর্ব উপ-হিমালয় পর্বতমালা থেকে উদ্ভব হয়েছে।